

**BEHAVIOR OF PILE GROUPS SUBJECTED
TO DYNAMIC LOADING**

By

Toyoaki Nogami, Associate Professor

and

Hsiao-Liang, Graduate Research Assistant

University of Houston
Houston, Texas

Presented at the Fourth Canadian Conference of Earthquake Engineering

BEHAVIOR OF PILE GROUPS SUBJECTED TO DYNAMIC LOADING

by

Toyoaki Nogami, Associate Professor, and
 Hsiao-Liang Chen, Graduate Research Assistant
 University of Houston, Dept. of Civil Engineering
 Houston, Texas 77004

ABSTRACT

A Winkler soil model for pile groups is described for both axial and flexural responses of pile groups subjected to dynamic loading. Using this soil model, closed form solutions of dynamic responses of pile groups are obtained. The responses of pile groups are reviewed for two-pile groups and the natures of pile-soil-pile interactions are studied. The frequency dependent parameters of the equivalent Kelvin-Voight model are shown for 2 x 4 piles attached to a common rigid cap.

INTRODUCTION

Several people have studied the dynamic responses of pile groups. Among them, Wolf and Von Arx (1978) used a finite element method. Nogami (1979) and Kaynia and Kausel (1982) used solutions obtained from equations for wave propagation in a three-dimensional continuum in their analyses of pile groups. Nogami (1980, 1982, and 1983) and Sheta and Novak (1982) developed a Winkler soil model for grouped piles which can account for a dynamic pile-soil-pile interaction in a Winkler model. The parameters of this Winkler model were defined from a solution obtained from equations of wave propagation in a plane strain medium.

This paper summarizes some of the findings obtained in the previous studies by the authors and also presents the new results on the dynamic response of pile groups.

SOIL MODEL

Two identical massless cylindrical columns are embedded in a homogeneous soil stratum as shown in Fig. 1. A perfect connection is assumed at the soil-pile interface. According to Refs. 2 and 3, the amplitude of the soil responses and soil reactions at the soil-column interface are expressed in the following forms under a steady state vibration; respectively

$$\begin{aligned} \{w\} &= \sum_n \{W_n\} \cos h_n z; \{p_v\} = \sum_n \{p_{vn}\} \cos h_n z && \text{vertical motion} \\ \{u\} &= \sum_n \{U_n\} \cos h_n z; \{p_h\} = \sum_n \{p_{hn}\} \cos h_n z && \text{lateral motion} \end{aligned} \quad (1)$$

where $\{w\}$ and $\{u\}$ = vectors containing the amplitudes of the two displacements; $\{p_v\}$ and $\{p_h\}$ = vectors containing the amplitudes of the two reaction forces; $h_n = \pi(2n - 1)/(2H)$; H = thickness of the stratum; and θ = direction of the force applied. The vectors in the right hand side of Eq. 1 are related to each other through $\{W_n\} = [f_{vn}]\{p_{vn}\}$ and $\{U_n\} = [f_{hn}]\{p_{hn}\}$ where $[f_{vn}]$ and $[f_{hn}]$ are 2 x 2 matrices and the value at the location (i,j) can be obtained from

$$f_{vn}(i,j) = \frac{K_0(\ell_n R)}{2\pi G_s^* r_0 K_1(\ell_n r_0)}$$

$$f_{hn}(i,j) = \frac{[K_1(q_n R) + q_n R K_0(q_n R)][2K_1(s_n r_0) + s_n r_0 K_0(s_n r_0)]}{\pi G_s^* r_0 R s_n^2 [4K_1(q_n r_0) K_1(s_n r_0) + s_n r_0 K_1(q_n r_0) K_0(s_n r_0) - K_1(s_n R)[2K_1(q_n r_0) + q_n r_0 K_0(q_n r_0)] + q_n r_0 K_0(q_n r_0) K_1(s_n r_0)]} \quad \dots \text{ for } \theta = 0^\circ$$

$$f_{hn}(i,j) = \frac{-K_1(q_n r_0)[2K(s_n r_0) + s_n r_0 K_0(s_n r_0)]}{\pi G_s^* r_0 R s_n^2 [4K_1(q_n r_0) K_1(s_n r_0) + [K_1(s_n R) + s_n r_0 K_0(s_n R)][2K_1(q_n r_0) + q_n r_0 K_0(q_n r_0)] + s_n r_0 K_1(q_n r_0) K_0(s_n r_0) + \frac{R}{r_0} K_1(q_n r_0) K(s_n r)]} \quad (2)$$

... for $\theta = 90^\circ$
 where $G_s^* = G_s(1+2iD_s)$; G_s = shear modulus of the soil; D_s = damping ratio of the soil; r_0 = radius of the pile; R = distance between the two piles for $i \neq j$ and $r = r_0$ for $i = j$; K_0 and K_1 are zero and the first order modified Bessel functions of the second kind, respectively; $\ell_n = \sqrt{(nh_n)^2 + (a\bar{g}/r_0)^2}$; $s_n = \sqrt{h_n^2 + (a\bar{g}/r_0)^2}$; $q_n = s_n/\eta$; $\eta = v_p/v_s$; v_p and v_s = P-wave and S-wave velocities, respectively; $a\bar{g} = a_0 i / \sqrt{1+2D_s}$; and $a_0 = r_0 \omega / v_s$. Thus, the soil stiffness matrix at the columns in the n -th mode can be obtained from $[k_{vn}] = [f_{vn}]^{-1}$ and $[k_{hn}] = [f_{hn}]^{-1}$ where $\{p_{vn}\} = [k_{vn}]\{W_n\}$ and $\{p_{hn}\} = [k_{hn}]\{U_n\}$.

When the frequency parameter a_0 is large compared to $\eta h_n r_0$, both ℓ_n and s_n can be replaced by $\ell_n = s_n = a\bar{g}/r_0$ and then the expressions in Eq. 2 become, respectively:

$$f_{vn}(i,j) = \frac{K_0(a_0^*)}{2\pi G_s^* a_0^* K_1(a_0^*)}$$

$$f_{hn}(i,j) = \frac{[K_1(b_0^* \bar{R}) + \bar{R} K_0(b_0^* \bar{R})][2K_1(a_0^*) + a_0^* K_0(a_0^*)] - K_1(a_0^* \bar{R})[2K_1(b_0^*) + b_0^* K_0(b_0^*)]}{\pi G_s^* \bar{R} a_0^*{}^2 [4K_1(b_0^*) K_1(a_0^*) + a_0^* K_1(b_0^*) K_0(a_0^*) + b_0^* K_0(b_0^*) K_0(a_0^*)]} \quad \dots \text{ for } \theta = 0^\circ$$

$$f_{hn}(i,j) = \frac{-K_1(b_0^*)[2K_1(a_0^*) + a_0^* K_0(a_0^*)] + [K_1(a_0^* \bar{R}) + a_0^* K_0(a_0^* \bar{R})][2K_1(b_0^*) + b_0^* K_0(b_0^*)]}{\pi G_s^* \bar{R} a_0^*{}^2 [4K_1(b_0^*) K_1(a_0^*) + a_0^* K_1(b_0^*) K_0(a_0^*) + b_0^* K_0(b_0^*) K_1(a_0^*)]} \quad \dots \text{ for } \theta = 90^\circ \quad (3)$$

where $b_0^* = a\bar{g}/r_0$; and $\bar{R} = R/r_0$. The expressions in Eq. 3 are independent of the mode number n and identical to those obtained under the plane strain conditions shown in Fig. 2. As the frequency a_0 increases beyond the fundamental natural frequency of the soil deposit, the stiffnesses $[k_{vn}]$ and $[k_{hn}]$ are found to approach quickly to the approximate expressions of those stiffnesses obtained from Eq. 3.

Using the approximate soil stiffness $[k_{v0}]$ constructed from Eq. 3, $\{P_v\}$ in Eq. 1 can be expressed approximately by $\{p_v\} = \sum_n [k_{v0}] \{W_n\} \cos h_n z \approx [k_{v0}] \sum_n \{W_n\} \cos h_n z$
 or $\{p_v\} \approx [k_{v0}]\{w\}$, and similarly $\{p_h\} \approx [k_{h0}]\{u\}$ (4)

The expressions in Eq. 4 indicate the soil reactions to the vibrating columns depend only on the displacements of the columns at the depth where the reactions are considered and are independent of those at other depths. Thus, the soil around the sides of the columns can be replaced by a Winkler model as shown in Fig. 3 and the parameters can be determined from the plane strain conditions shown in Fig. 2. Errors induced by this approximation in the soil model are very small and negligible for pile group problems at the frequencies higher than the fundamental natural frequency of the soil deposit (Fig. 4).

DYNAMIC RESPONSES OF PILE GROUPS

TWO-PILE GROUPS - The upper and lower portions of the columns shown in Fig. 1 are assumed to be occupied by the pile shaft and soil columns as shown in Fig. 5, respectively. The columns and the surrounding soil are divided into M segments and homogeneous soil layers. The equations of motions of the two columns for a steady state vibration can be written by

$$[EA] \frac{d^2}{dz^2} \{w\} + \omega^2 [m] \{w\} = \{P_v\} \quad (5)$$

$$-[EI] \frac{d^4}{dz^4} \{u\} + \omega^2 [m] \{u\} = \{P_h\}$$

where $[EA]$, $[EI]$, and $[m] = 2 \times 2$ diagonal axial stiffness, flexural stiffness, and mass matrices of the columns; and $\omega =$ circular excitation frequency. When the soil around the sides of the columns are replaced by a Winkler model as shown in Fig. 3, the solutions of Eq. 5 are:

$$\begin{aligned} \{w\} &= \sum_{j=1}^2 A_{vj} \exp(\lambda_{vj}z) \{d_{vj}\} + B_{vj} \exp(-\lambda_{vj}z) \{d_{vj}\} \\ \{u\} &= \sum_{j=1}^2 A_{hj} \exp(\lambda_{hj}z) \{d_{hj}\} + B_{hj} \exp(-\lambda_{hj}z) \{d_{hj}\} \\ &\quad + C_{hj} \exp(i\lambda_{hj}z) \{d_{hj}\} + D_{hj} \exp(-i\lambda_{hj}z) \{d_{hj}\} \end{aligned} \quad (6)$$

where λ_{vj} and $\{d_{vj}\} = j$ -th eigenvalue and eigenvector for axial response, respectively; and λ_{hj} and $\{d_{hj}\} = j$ -th eigenvalue and eigenvector for flexural response, respectively. The above eigenvalues and eigenvectors are obtained from the following equations:

$$[\lambda_v^2 [I] + [\gamma_v]] \{d_v\} = \{0\} \quad \text{or} \quad [\lambda_h^4 [I] - [\gamma_h]] \{d_h\} = \{0\} \quad (7)$$

where $[Y_V] = [EA]^{-1} [\omega^2[m] - [k_{VO}]]$; $[Y_H] = [EI]^{-1} [\omega^2[m] - [k_{HO}]]$; $[k_{VO}]$ and $[k_{HO}]$ = soil stiffness matrices obtained under the plane strain conditions for vertical and lateral soil reactions, respectively. From Eq. 6 and the conditions shown in Fig. 6, the displacements and forces at the upper end of the segment are related with those at the bottom end through the expression,

$$\begin{Bmatrix} \{w\} \\ \{P_V\} \end{Bmatrix}_j = [t_{Vj}] \begin{Bmatrix} \{w\} \\ \{P_V\} \end{Bmatrix}_{j+1} \quad \text{and} \quad \begin{Bmatrix} \{u\} \\ \{\psi\} \\ \{P_H\} \\ \{M\} \end{Bmatrix}_j = [t_{Hj}] \begin{Bmatrix} \{u\} \\ \{\psi\} \\ \{P_H\} \\ \{M\} \end{Bmatrix}_{j+1} \quad (8)$$

where $\{P_V\}$ and $\{P_H\}$ = amplitudes of axial and shear forces in the columns, respectively; $\{M\}$ = amplitudes of moment forces in the columns; $\{\psi\}$ = amplitudes of rotations of the columns; and $[t_{Vj}]$ and $[t_{Hj}]$ = transfer matrices within the j-th segment. The relationship in Eq. 8 for $j=1$ through $j=M$ leads to

$$\begin{Bmatrix} \{w\} \\ \{P_V\} \end{Bmatrix}_1 = [T_V] \begin{Bmatrix} \{w\} \\ \{P_V\} \end{Bmatrix}_{M+1} \quad \text{and} \quad \begin{Bmatrix} \{u\} \\ \{\psi\} \\ \{P_H\} \\ \{M\} \end{Bmatrix}_1 = [T_H] \begin{Bmatrix} \{u\} \\ \{\psi\} \\ \{P_H\} \\ \{M\} \end{Bmatrix}_{M+1} \quad (9)$$

where $[T_V] = [t_{V1}] [t_{V2}] \dots [t_{VM}]$; and $[T_H] = [t_{H1}] [t_{H2}] \dots [t_{HM}]$

The zero displacement boundary conditions at the bottom of the soil stratum lead to

$$\{w\}_1 = [F_{wp}] \{P_V\}_1; \quad \begin{Bmatrix} \{u\} \\ \{\psi\} \end{Bmatrix}_1 = \begin{bmatrix} [F_{up}] & [F_{uM}] \\ [F_{\psi p}] & [F_{\psi M}] \end{bmatrix} \begin{Bmatrix} \{P_H\} \\ \{M\} \end{Bmatrix}_1 \quad (10)$$

where $[F] = [T_{12}] [T_{22}]^{-1}$; and $[T_{12}]$ and $[T_{22}]$ = 2 x 2 submatrices for axial response or 4 x 4 submatrices for flexural response, located in the following positions of $[T]$:

$$[T] = \begin{bmatrix} [T_{11}] & [T_{12}] \\ [T_{21}] & [T_{22}] \end{bmatrix}$$

GENERAL PILE GROUPS - N piles in a group and the global coordinates, x y z, are shown in Fig. 7. Using a plane strain assumption, the soil stiffness matrix for N piles can be expressed in a similar way as that described above,

$$\{p_z\} = [k_V] \{\delta_z\} \quad \text{and} \quad \begin{Bmatrix} \{p_x\} \\ \{p_y\} \end{Bmatrix} = [k_H] \begin{Bmatrix} \{\delta_x\} \\ \{\delta_y\} \end{Bmatrix} \quad (11)$$

where $\{\delta_x\}$, $\{\delta_y\}$ and $\{\delta_z\}$ = vectors containing amplitudes of the N displacements in the x, y and z directions, respectively; $\{p_x\}$, $\{p_y\}$ and $\{p_z\}$ = vectors containing amplitudes of the N soil reactions in the x, y and z directions, respectively; $[k_v]$ and $[k_h]$ = soil stiffness matrices in the global coordinate system.

Using the notations corresponding to the global coordinate system and Eq. 11, the equation of motion in Eq. 5 can be rewritten for the global coordinate system. The matrix $[T]$ is obtained by solving this equation following the same procedures as those described above. Then, the pile-head stiffness matrix of N-grouped piles is $[K] = [T_{22}] \times [T_{12}]^{-1}$ where $[T_{22}]$ and $[T_{12}]$ are N x N matrices for axial response, and 2N x 2N matrices for flexural response; and the stiffness matrices $[K]$ for axial and flexural responses are defined by, respectively

$$\{p_z\} = [K] \{\delta_z\} \quad \text{and} \quad \begin{Bmatrix} \{P_x\} \\ \{M_y\} \\ \{P_y\} \\ \{M_x\} \end{Bmatrix} = [K] \begin{Bmatrix} \{\delta_x\} \\ \{\phi_y\} \\ \{\delta_y\} \\ \{\phi_x\} \end{Bmatrix} \quad (12)$$

where $\{\phi_y\}$ and $\{M_y\}$ = vectors containing amplitudes of N rotations and moments around the y axis, respectively; $\{\phi_x\}$ and $\{M_x\}$ = vectors containing amplitudes of N rotations and moments around x axis, respectively.

When the piles are arranged symmetrically with respect to the x and y axes and attached to a common rigid cap, the stiffnesses of the piles and cap system at the center of the origin of the coordinates are expressed by

$$P_z = K_{p\delta}^{cap} \delta_z \quad \text{and} \quad \begin{Bmatrix} P_j \\ M_i \end{Bmatrix} = \begin{bmatrix} K_{p\delta}^{cap} & K_{p\phi}^{cap} \\ K_{M\delta}^{cap} & K_{M\phi}^{cap} \end{bmatrix} \begin{Bmatrix} \delta_j \\ \phi_i \end{Bmatrix} \quad (13)$$

where $j = x$ and $i = y$ for the motions on $\beta = 0^\circ$ plane, and $j = y$ and $i = x$ for the motions on $\beta = 90^\circ$ plane; stiffness in Eq. 13 can be obtained from $[K]$ in Eq. 12.

The pile groups attached to a rigid cap are often modeled by a Kelvin-Voigt model. The parameters of this model are defined by $k^{cap} = \text{Re } K^{cap}$ and $c^{cap} = \text{Im } K^{cap}/\omega$ where k^{cap} and c^{cap} = spring and dashpot parameters in an equivalent Kelvin-Voigt model.

RESULTS AND REVIEW

The diagonal terms of the pile-head flexibility matrix are nearly identical to the flexibility of a single isolated pile. Thus, the group factor can be determined using the flexibility matrix in Eq. 10 by

$$\text{group factor} = \frac{\text{amplitude of } F_j(1,2)}{\text{amplitude of } F_j(1,1)}$$

where $j = wP, uP, uM, \psi P$ or ψM . Figure 8 shows the comparison between the static and dynamic group factors for various distances of pile

spacing between the two piles. The relative stiffness between pile and soil, K_R , is defined here by $K_R = (EA)/(E_s L^2)$ for axial stiffness and $K_R = (EI)/(E_s L^4)$ for flexural stiffness where L is the length of the pile. It is seen in the figure that the dynamic conditions increase the group effect more for more flexible piles and for $\theta = 90^\circ$ than for $\theta = 0^\circ$. These trends are most significant in the coupling terms, $F_{\psi p}$ and F_{UM} .

The dynamic response of pile groups is affected by not only the amplitude but also the phase shift of the motions transmitted from other piles. Figure 9 shows the variation of both the amplitude and phase shift of the pile response induced by the other pile in two-pile group. Both homogeneous and non-homogeneous soil profiles were used in this study. The distribution of Young's modulus in the non-homogeneous soil profile is defined in Fig. 10. The average soil properties along the pile shaft length in the nonhomogeneous soil profile correspond to those in the homogeneous soil profile. Figure 9 shows that the amplitude of the pile response induced by the transmitted motion decreases more rapidly with distance in the nonhomogeneous soil profile than the homogeneous profile, whereas the phase shift increases more rapidly with distance in the nonhomogeneous soil profile.

The material damping decreases the amplitude of the transmitted motion. This trend is more pronounced in $\theta = 90^\circ$ than $\theta = 0^\circ$ in flexural response. The phase shift of the response induced by the transmitted motion in the $\theta = 90^\circ$ flexural response is very similar to that in axial response, and varies with distance more rapidly than the phase shift in the $\theta = 0^\circ$ flexural response. This is because the motion is governed by the S-wave in both axial and $\theta = 90^\circ$ flexural responses and by the P-wave in the $\theta = 0^\circ$ flexural response.

Because of the difference in the phase shift between the pile responses induced by direct loading and by the transmitted motion, the behaviors of the spring and dashpot parameters of the pile group differ from those of a single isolated pile as shown in Fig. 11; where the curve "no group effect" shows the behaviors of a single isolated pile. The peak value occurs when the phase shift between the $F_j(1,1)$ and $F_j(1,2)$ is equal to π .

When the 2 x 4 piles attached to a rigid cap shown in Fig. 12 is considered, the spring and dashpot parameters vary with frequency as shown in Fig. 13. The behaviors of these parameters result from the superposition of the transmitted motions from all the piles through the soil medium.

CONCLUSIONS

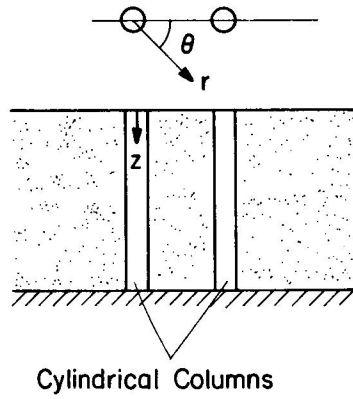
For the analysis of dynamic response of pile groups, the soil around the pile shafts can be reasonably well modeled as a Winkler model. This Winkler model for the pile group can be defined from the behavior of a plane strain medium, and is capable of reproducing the pile-soil-pile interaction.

The dynamic response of pile groups results from the superposition between the pile responses directly induced and induced by the transmitted motions from other piles in a group through the wave motion in the soil medium. The behaviors of the pile groups is generally more strongly frequency dependent than that of single piles.

This is due to the phase shifts between the directly induced pile motion and the transmitted motions. Thus, the frequency dependent behavior of pile groups is controlled by the type of predominant waves induced in the soil, frequency, and distance of pile spacing. The effect of the soil material damping is primarily a reduction of the amplitude of the transmitted motion. Gibson type nonhomogeneity in the soil profile tends to decrease the amplitude but increase the phase shift of the transmitted motion from those values corresponding to a homogeneous soil profile.

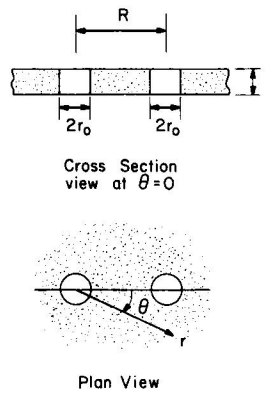
REFERENCES

1. Kaynia, A.M., and Kausel, E., "Dynamic Behavior of Pile Groups," Proceedings, Second International Conference on Numerical Methods in Offshore Piling, I.C.E., 1982.
2. Nogami, T., and Novak, M., "Soil-Pile Interaction in Vertical Vibration," International Journal of Earthquake Engineering and Structural Dynamics, Vol. 4, No. 3, 1976, pp. 277-293.
3. Nogami, T., and Novak, M., "Resistance of Soil to Horizontally Vibrating Piles," International Journal of Earthquake Engineering and Structural Dynamics, Vol. 5, No. 3, 1977, pp. 249-262.
4. Nogami, T., "Dynamic Group Effect of Multiple Piles Under Vertical Vibration," Proceedings of Third ASCE Engineering Mechanics Specialty Conference, Austin, Texas, 1979.
5. Nogami, T., "Dynamic Stiffness and Damping of Pile Groups in Inhomogeneous Soil," ASCE Special Technical Publication on Dynamic Response of Pile Foundations: Analytical Aspect, 1980, pp. 31-52.
6. Nogami, T. and Chen, H.L., "Flexural Responses of Grouped Piles under Dynamic Loading," Civil Engineering Report, No. GT-TN11-82, University of Houston, Dec., 1982.
7. Nogami, T., "Dynamic Group Effect in Axial Responses of Grouped Piles," Journal of Geotechnical Engineering, ASCE, Vol. 109, No. GT2, 1983.
8. Sheta, M., and Novak, M., "Vertical Vibration of Pile Groups," Journal of the Geotechnical Engineering Division, ASCE, Vol. 108, No. GT4; 1982, pp. 570-590.
9. Wolf, J., and Von Arx, G.A., "Impedance Function of a Group of Vertical Piles," Proceedings of ASCE Geotechnical Engineering Specialty Conference, Pasadena, 1978, pp. 1024-1041.



Cylindrical Columns

Fig. 1. Two Cylindrical Columns in Soil Medium



Cross Section view at $\theta=0$

Plan View

Fig. 2. Plane Strain Soil Model

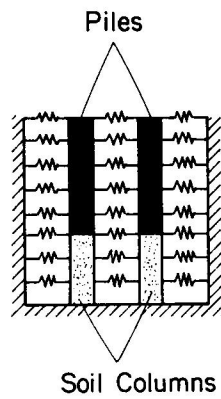


Fig. 3. Winkler Model and Column system

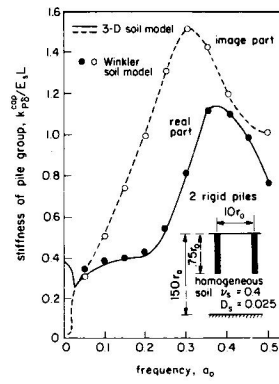


Fig. 4. Comparison Between Winkler and 3-D Models

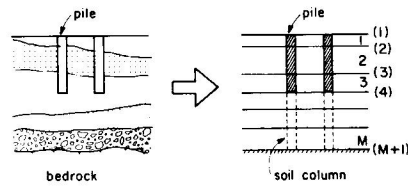


Fig. 5 Divided Soil-Pile System

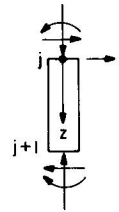
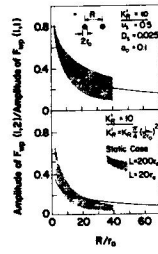
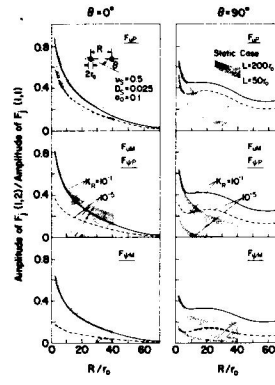


Fig. 6. Forces Acting on Segment

Fig. 7. Global Coordinate System

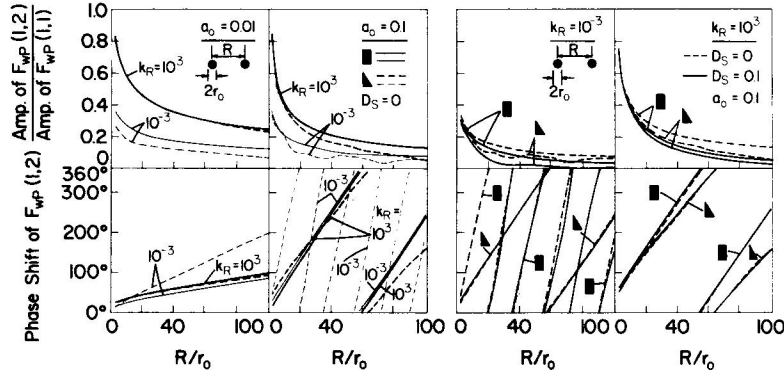


(a) Axial Pile Response

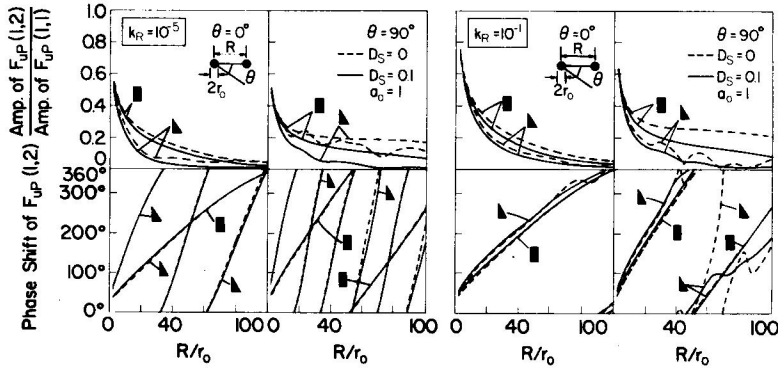


(b) Flexural Pile Response

Fig. 8. Static and Dynamic Group Factors



(a) $F_{wp}(1,2)$ for Various D_s and K_R



(b) $F_{up}(1,2)$ for Various D_s and K_R

Fig. 9. Dynamic Group Factors for Various Conditions

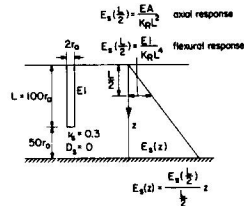


Fig. 10. Nonhomogeneous Soil Profile

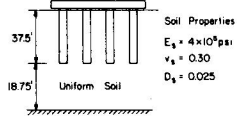
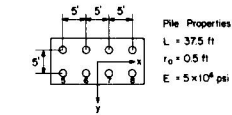


Fig. 12. Pile Group and Soil Properties

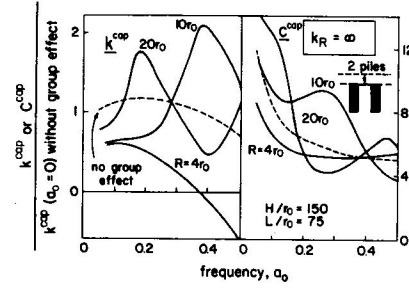
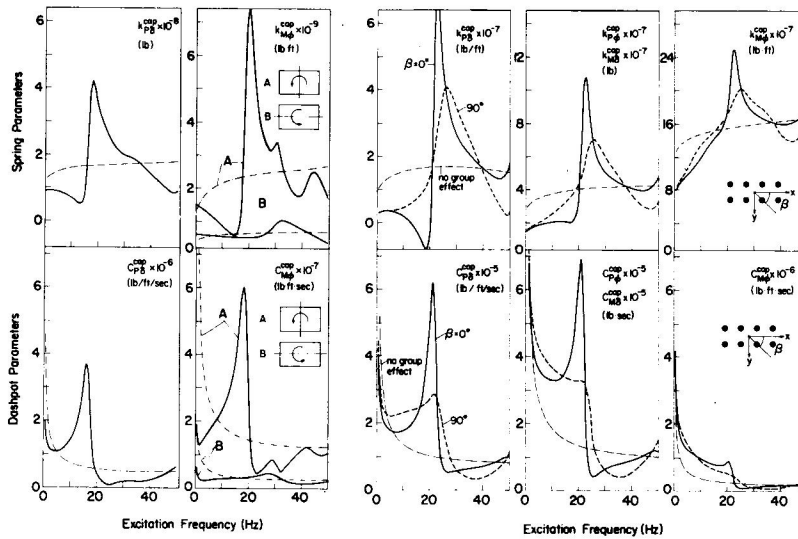


Fig. 11. Parameters of Pile Groups at Various Frequencies



(a) Axial Response

(b) Flexural Response

Fig. 13. Parameters of Pile Groups at Various Frequencies